Supplementary Materials and Methods

Cell lines and cell culture. In this study, human HCC cell lines, PLC/PRF5, Hep3B and HepG2 cells were purchased from the American Type Culture Collection (ATCC, Manassas, VA). MHCC97-L, MHCC97-H and HCCLM3 were kindly provided by the Liver Cancer Institute of Fudan University, Shanghai, China, where these cell lines were established. SMMC7721, Huh7 and immortalized human normal liver cells L02 were purchased from the Cell Bank of Typical Culture Preservation Committee of Chinese Academy of Science, Shanghai, China. Cell culture was according to the manufacturer's protocol and all the cell lines grow at 37℃ with 5% CO_2. The cells' metastatic potential and features statements were according to previous studies (1-5).

RNA extraction and semi-quantitative RT-PCR. TRIzol® Reagent (Life Technologies, Carlsbad, CA) was used to isolate total RNA from frozen patient samples and cell lines according to the manufacturer's protocol. cDNA was synthesized using the universal cDNA synthesis kit (Toyobo, tokyo, JP). The RNA was then reverse-transcribed to obtain cDNA by the universal cDNA synthesis kit (Toyobo, tokyo, JP) at 37°C for 50 min. PCR products were separated by electrophoresis on 1.2% agarose gels and were visualized under ultraviolet light after ethidium bromide staining. All quantifications were normalized to the level of endogenous GAPDH as a control. The detailed procedure was according to previously described (6). The primer sequences

are listed in the Supplementary Table 4.

Real-Time Quantitative Polymerase Chain Reaction (qRT-PCR). The cDNA was subjected to quantitative real-time PCR (qRT-PCR) using the SYBR Green PCR Kit (Roche Life Sciences, Switzerland) and the assay was performed on an PRISM 7300 Sequence Detection System (Applied Biosystems, CA). GAPDH was used as an internal control. The relative levels of expression were quantified and analyzed. The experiments were done in triplicate. The primers were all synthesized and bought from Invitrogen Company (Shanghai, China). The primer sequences are listed in the Supplementary Table 4.

Western Blot. Total proteins were extracted with RIPA lysis buffer and separated by SDS-PAGE and then transferred to the PVDF membrane (Roche Life Sciences, Switzerland). The membrane were blocked with 5% skimmed milk and incubated with the appropriate antibody. The antigen-antibody complex on the membrane was detected with enhanced chemiluminescence regents (Thermo Scientific, Waltham, MA). The antibodies are listed in the Supplementary Table 5.

Immunohistochemistry. Immunohistochemical staining for tissue was performed using the polymer HRP detection system (Zhongshan Goldenbridge

Biotechnology) on formalin-fixed, paraffin-embedded tissue sections that had been cut to 4-μm thickness as described previously (7). The paraffin sections were dewaxed and antigen retrieval with 0.01 M sodium citrate buffer (pH 6.0), followed with 3 % hydrogen peroxide incubated for 20 min at room temperature to block endogenous peroxidase, next with 10 % donkey serum blocking for 30 min. Primary antibodies were incubated overnight at 4 ℃ in a humidified chamber, followed by HRP conjugated secondary antibody incubation for 30 minutes at room temperature. Antibody binding was detected by DAB and reaction was stopped by immersion of tissue sections in distilled water once brown color appeared. Tissue sections were counterstained by hematoxylin, dehydrated in graded ethanols and mounted. Appropriate positive and negative controls were included for each run of IHC. The antibodies were listed in the Supplementary Table 5.The immunohistochemical staining was scored according to the percentage of positived stained tumor cells, with 0 denotes less than 5% of tumor cells stained positive, 1 denotes 5 – 30%, 2 denotes 31 – 50%, 3 denotes 51 – 80% and 4 denotes >80% of tumor cells stained positive (8). The protein expression in HCC specimens was also divided into a low expression group (0 - 1) and a high expression group (2 - 4) for further analysis.

Immunofluorescence The tissues immunofluorescence was according to the protocol of Abcam. Immunofluorescence for cells, cells growth at glass

coverslips, and then fixed with 4% paraformaldehyde in phosphate-buffered saline (PBS) with 0.2% Trion. Cells were then blocked for an hour with 1% bovine serum albumin (BSA) followed by incubation with primary antibody overnight at 4°C. Cells were washed and incubated with appropriate secondary antibody and DAPI. The protocol of immunofluorescence for tissues were similar to IHC-P without 3 % hydrogen peroxide incubated, followed with mixed primary antibodies, next with mixed dylight-tagged secondary antibodies. The antibodies are listed in the Supplementary Table 5 and 6.

Chromatin Immunoprecipitation (ChIP) assay. ChIP assays were performed using the EpiQuik™ Chromatin Immunoprecipitation Kit (P-2002, Epigentek, NY) according to the manufacturer's protocol. Briefly, HCC cells were collected and fixed for 10 min at room temperature with 1% formaldehyde, followed in sequence with cell lysis and DNA shearing, Protein and DNA immunoprecipitation, cross-linked DNA reversal and DNA purification, and finally the immunoprecipitated DNA fragments were detected by real-time PCR assays using appropriate primers. All assays were repeated three times. The normal mouse IgG was used as the negative control, and anti-RNA polymerase II as the positive control. The primers were listed in the Supplementary table 7.

Establishment of ACTL6A overexpression and knockdown cells. ACTL6A

ectopic expression and knockdown lentivirus as well as their negative control (NC) lentivirus were purchased from GeneChem (Shanghai, China). Full-length human ACTL6A ectopic expression lentivirus was transfected into PLC/PRF5 cells, and lentiviral containing short hairpin RNAs (shRNA) targeting ACTL6A was transfected into Hep3B cells according to the manufacturer's instructions. Cells transfected with empty vector were used as controls. Puromycin (final concentration: 2μg/ml) was used to select stable clones. The sequences of RNAi and cDNA clone are listed in the Supplementary Table 8.

MTT assay and colony formation assay. To determine the level of cell proliferation, cells were seeded into each well of 96-well plates at a density of 5 × 10^3 cells/well. Six wells of each group were detected every day. 100 μl fresh medium containing MTT (Sigma, St Louis, MO) 0.5 mg/ml was put into each cell and incubated at 37°C for 4hrs, then the medium was replaced by 100 μl of DMSO and shaken at room temperature for 10 mins. The absorbance was measured at 570 nm. For colony formation assays, cells were seeded into 35mm dishes (Corning, NY) at a density of 5 × 10^2 cells/dish and cultured for 2 weeks at 37°C. The numbers of colonies per dish were counted after staining with crystal violet. All studies were conducted with 3 replicates.

MTS assay. Dispense 5× 10^3 per cells into wells of the 96-well plates in a final

volume of 100 µl. Incubate the plate at 37 °C for 48–72 hours in a humidified, 5% CO_2 atmosphere. Add 20 µl per well of CellTiter 96® AQueous One Solution Reagent. Incubate the plate at 37 °C for 1–4 hours in a humidified, 5% CO_2 atmosphere. Record the absorbance at 490nm using a 96-well plate reader. Each experiment was conducted with 3 replicates (9).

Anchorage-independent growth assay. Cells were seeded at 5×10^3 cells per well in a six-well plate containing 0.3% low melting temperature soft agar (Sigma, St. Louis, MO). Cultures were fed with fresh media every 4 days. Colonies were observed under phase contrast microscope, counted and measured after 14 days (10).

In vitro migration assay. Cell migration was measured using a cell wound-healing assay in six-well plates in culture medium containing DMEM with 10% FBS. When cells grew to 90% confluence, they were preincubated with Mitomycin-C (10 µg/ml) for 1h at 37 °C to suppress cell proliferation, next rinsed with phosphate-buffered saline (PBS), and then starved for 24 hours in serum-free medium. A sterile 10 µL pipette tip was used to create three separate, parallel wounds, and migration of the cells across the wound line was assessed after 24 or 48 hours (11, 12). These experiments were performed in triplicate.

In vitro invasion assay. Cells in culture dish were preincubated with Mitomycin-C (10 μg/ml) for 1h at 37 °C to suppress proliferation, then 1×10^5 cells in serum-free medium containing 0.1% bovine serum albumin were placed into the upper chamber of the insert with matrigel (BD Biosciences, MA). After 12-48 hours of incubation at 37°C, the cells remained in the upper chamber or on the upper membrane were removed. The number of cells adhering to the lower membrane of the inserts was counted after staining with a solution containing 0.1% crystal violet and 20% methanol. The numbers of cells was counted under an inverted microscope (Nikon).

HCC mouse model. The hepatocellular carcinoma model in nude mice was constructed as described before (13, 14). Briefly, 5×10^6 HCCLM3 cells were injected subcutaneously into the left upper flank regions of nude mouse (3-4 weeks of age, male, BALB/c). The subcutaneous tumor size was calculated and recorded every week used vernier caliper as follows: tumor volume (mm^3) = $(L \times W^2)/2$, where L = long axis and W = short axis, the measurements were repeated three times. The subcutaneous tumor tissues were removed and calculated 6 wks later. Then the subcutaneous tumor was cut into pieces of the same size as 1 mm^3, and implanted into the liver of each group respectively to mimic the primary HCC (6 in each group). After 8 wks of implantation, the mice were sacrificed, and the size for tumors was calculated and compared as mentioned above. Livers and lungs were harvested and fixed with

phosphate-buffered neutral formalin. Serial sections were subjected to histopathological analysis by hematoxylin and eosin (H&E) staining, the metastatic foci was confirmed and recorded by specialized pathologists. Then, the overall metastasis rate of tumors generated from each cell line was compared between the groups of each panel. All animal studies were conducted in the Animal Institute of CSU according to the protocols approved by the Medical Experimental Animal Care Commission of CSU.

Statistical analysis. Statistical analyses were performed using SPSS 17.0 for Windows (SPSS) and Graphpad Prism6. Data were expressed as the mean ± standard error of the mean (SEM) from at least three independent experiments. Quantitative data between groups were compared using the Student *t* test. Categorical data were analyzed by the c2 test or Fisher exact test. Correlations between different protein expressions level were determined using Spearman's rank analysis. Overall survival and disease-free survival curves were obtained by the Kaplan-Meier method, and differences were compared by the log-rank test. Univariate analysis and multivariate analysis were analyzed with Cox proportional hazard regression model to verify the independent risk factors. A two-tailed *P* value of less than 0.05 was considered as statistical significance.

Supplementary References：

1. Bertran E, Crosas-Molist E, Sancho P, Caja L, Lopez-Luque J, Navarro E, et al. Overactivation of the TGF-beta pathway confers a mesenchymal-like phenotype and CXCR4-dependent migratory properties to liver tumor cells. Hepatology,2013,58:2032-2044.

2. Zhou Y M, Cao L, Li B, Zhang R X, Sui C J, Yin Z F, et al. Clinicopathological significance of ZEB1 protein in patients with hepatocellular carcinoma. Ann Surg Oncol,2012,19:1700-1706.

3. Chung K Y, Cheng I K, Ching A K, Chu J H, Lai P B, Wong N. Block of proliferation 1 (BOP1) plays an oncogenic role in hepatocellular carcinoma by promoting epithelial-to-mesenchymal transition. Hepatology,2011,54:307-318.

4. Tang Z Y, Ye S L, Liu Y K, Qin L X, Sun H C, Ye Q H, et al. A decade's studies on metastasis of hepatocellular carcinoma. J Cancer Res Clin Oncol,2004,130:187-196.

5. Tian J, Tang Z Y, Ye S L, Liu Y K, Lin Z Y, Chen J, et al. New human hepatocellular carcinoma (HCC) cell line with highly metastatic potential (MHCC97) and its expressions of the factors associated with metastasis. Br J Cancer,1999,81:814-821.

6. Chang R M, Yang H, Fang F, Xu J F, Yang L Y. MicroRNA-331-3p promotes proliferation and metastasis of hepatocellular carcinoma by targeting PH domain and leucine-rich repeat protein phosphatase. Hepatology,2014,60:1251-1263.

7. Wu F, Yang L Y, Li Y F, Ou D P, Chen D P, Fan C. Novel role for epidermal

growth factor-like domain 7 in metastasis of human hepatocellular carcinoma. Hepatology,2009,50:1839-1850.

8. Yong K J, Gao C, Lim J S, Yan B, Yang H, Dimitrov T, et al. Oncofetal gene SALL4 in aggressive hepatocellular carcinoma. N Engl J Med,2013,368:2266-2276.

9. Wang X, Zhang C, Yan X, Lan B, Wang J, Wei C, et al. A novel bioavailable BH3 mimetic efficiently inhibits colon cancer via cascade effects of mitochondria. Clin Cancer Res,2015. pii: clincanres.0732.2015.

10. Franken N A P, Rodermond H M, Stap J, Haveman J, van Bree C. Clonogenic assay of cells in vitro. Nature Protocols,2006,1:2315-2319.

11. Pullar C E, Chen J, Isseroff R R. PP2A activation by beta2-adrenergic receptor agonists: novel regulatory mechanism of keratinocyte migration. J Biol Chem,2003,278:22555-22562.

12. Fang F, Chang R M, Yu L, Lei X, Xiao S, Yang H, et al. MicroRNA-188-5p suppresses tumor cell proliferation and metastasis by directly targeting FGF5 in hepatocellular carcinoma. J Hepatol,2015,63:874-885.

13. Yang H, Fang F, Chang R, Yang L. MicroRNA-140-5p suppresses tumor growth and metastasis by targeting transforming growth factor beta receptor 1 and fibroblast growth factor 9 in hepatocellular carcinoma. Hepatology,2013,58:205-217.

14. Lu X, Qin W, Li J, Tan N, Pan D, Zhang H, et al. The growth and metastasis of human hepatocellular carcinoma xenografts are inhibited by

small interfering RNA targeting to the subunit ATP6L of proton pump. Cancer Res,2005,65:6843-6849.

Supplementary Figure legends:

Supplementary Figure 1. **Flow chart of HCC patients enrolled in this study.**

Supplementary figure 2. ACTL6A expression was associated with metastasis of HCC. (A) Representative IHC images of ACTL6A protein expression in adjacent non-tumor liver tissue, no-metastasis tumor tissue and metastasis tumor tissue. Magnification of upper panel was 100×, magnification of lower panel was 400×. (B) ACTL6A expression in small HCC (SHCC), SLHCC, solitary large HCC (SLHCC) and nodular HCC (NHCC) was detected by real-time PCR, which showed NHCC had the highest ACTL6A expression.

Supplementary figure 3. ACTL6A high expression associates with poor survival according to different clinical subtypes of HCC. (A) Kaplan-Meier curves indicated high ACTL6A associated with shorter OS and DFS of HCC in the overall cohort. (B) Kaplan-Meier curves indicated high ACTL6A associated with shorter OS and DFS of SHCC, (C) SLHCC, and (D) NHCC patients after liver resection.

Supplementary figure 4. ACTL6A promoted HCC cells proliferation and invasion *in vitro*. (A) Real-time PCR and (B) western blot identified the mRNA and protein expression of ACTL6A in PLC/PRF5-ACTL6A cells, Hep3B-shACTL6A-1,-2,-3 cells and their control cells. (C) The colony formation, (D) trans-well and (E) wound-heal assays indicated ACTL6A ectopic expression promoted proliferation, migration and invasion in vitro, while ACTL6A knockdown had the opposite effects.

Supplementary figure 5. ACTL6A promoted HCC growth in vivo. (A) The growth curves of mouse subcutaneous transplanted tumors generated from PLC/PRF5-ACTL6A, Hep3B-shACTL6A and their control cells were detected and compared. (B) ACTL6A expression in orthotopic transplanted tumors was confirmed by IHC. Upper panel magnification: 100×, lower panel magnification: 400×.

Supplementary figure 6. The expressions of EMT markers are determined in HCC cells. (A) The expressions of ACTL6A, epithelial marker (E-cadherin) and mesenchymal markers (vimentin, snail) in PLC/PRF-ACTL6A and PLC/PRF5 cells were detected by real-time PCR. (B) The expressions of ACTL6A, E-cadherin, vimentin and snail were detected in Hep3B-shACTL6A and Hep3B cells.

Supplementary figure 7. The cut-off value of DAPT treatment is determined in HCC cells. (A) MTS assay analysis of cell relative viability of ACTL6A-interfered cells and their control cells with DMSO or different DAPT dosage treatment for 72 hours. (B) NICD1 expression levels after DMSO or different DAPT dosage treatment for 72 hours in Hep3B and PLC/PRF5-ACTL6A cells.

Supplementary figure 8. ACTL6A promotes migration, invasion and anchor-independent growth of HCC cells through Notch signaling. (A) Wound-heal assay analyzed the migration capacity of ACTL6A-interfered cells and their control cells with/without DAPT treatment. (B) Trans-well assay analyzed the invasion capacity of ACTL6A-interfered cells and their control cells with/without DAPT treatment. (C) Anchor-independent growth assay analyzed the migration capacity of ACTL6A-interfered cells and their control cells with/without DAPT treatment.

Supplementary figure 9. The efficacy of SOX2 silence or ectopic expression is determined in ACTL6A-mediated HCC cells. (A) Real-time PCR and (B) western blot confirmation of SOX2 mRNA and protein expression in SOX2 knockdown PLC/PRF5-ACTL6A cells, SOX2 ectopic expression Hep3B-shACTL6A cells and their control cells.

Supplementary figure 10. SOX2 promotes migration and invasion of ACTL6A-interfered HCC cells. (A) SOX2 knockdown decreased the wound-healing area and invasion cell numbers of PLC/PRF5-ACTL6A cells. (B) SOX2 ectopic expression increased the wound-healing area and invasion number of Hep3B-shACTL6A cells.

Supplementary figure 11. The expression of ACTL6A, NICD1 and SOX2 in HCC samples. (A) Representative IHC images showed ACTL6A, SOX2 and NICD1 were co-location in consecutive sections of HCC sample. (B) Correlation analysis revealed the positive correlation of ACTL6A, SOX2 and NICD1 expression in training and validation cohorts.

Supplementary figure 12. ChIP-qPCR assay analysis of the direct binding of ACTL6A to the SOX2 promoter, and SOX2 to the Notch1 promoter. (A) Positions of primers for the promoter regions of SOX2 and Notch1 are shown. (B) ChIP-qPCR assay was performed using antibody against endogenous ACTL6A or SOX2 showed ACTL6A bound to the SOX2 promoter regions (left panel); and SOX2 bound to the Notch1 promoter proximal regions (left panel).

Supplementary figure 13. Immunohistochemistry analysis of cytokeratin 19 expression in HCC. Representative IHC images of cytokeratin 19 negative

expression in ANLT, low and high expression in tumor tissue. Magnification of upper panel was 100×, magnification of lower panel was 400×.

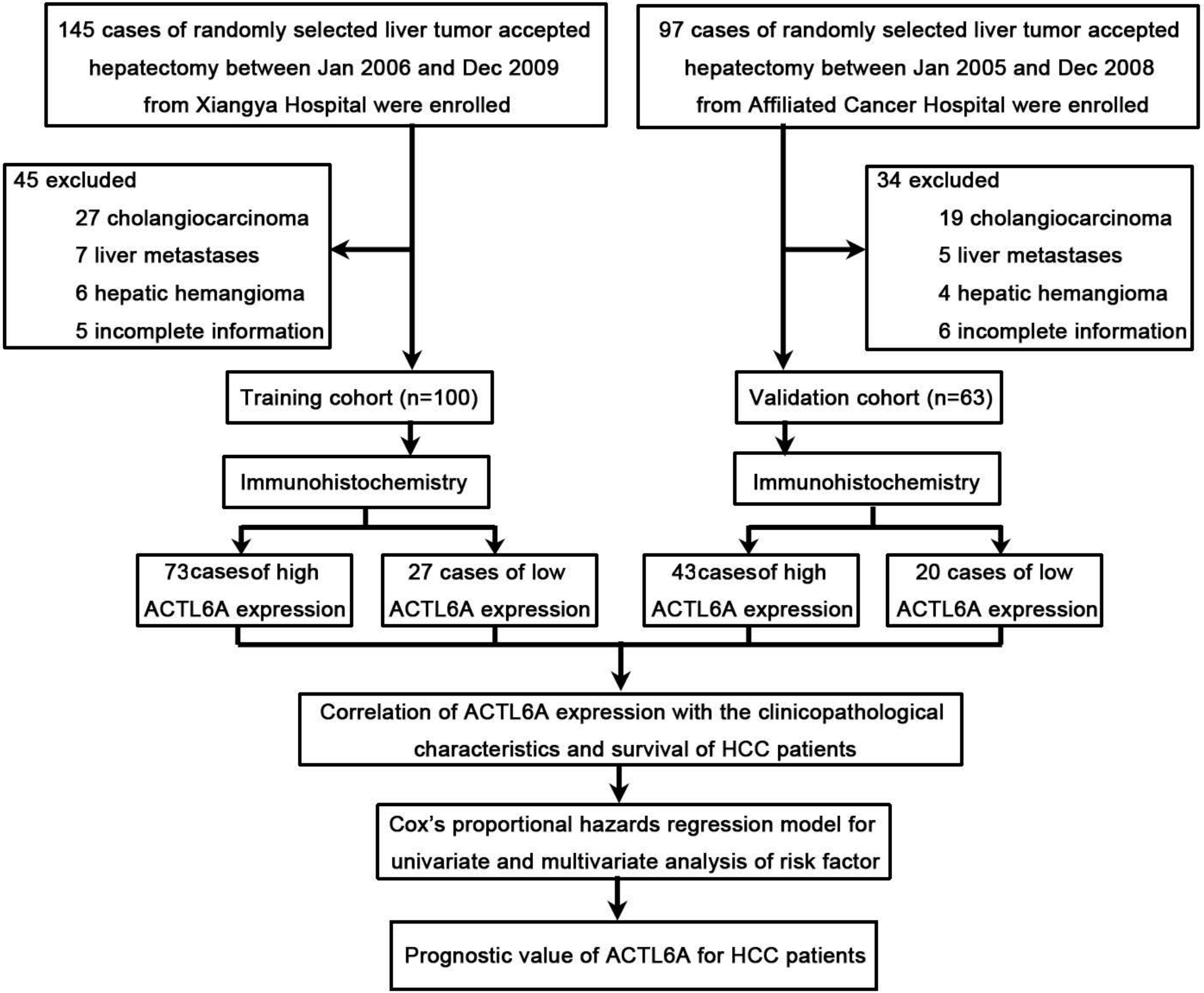
145 cases of randomly selected liver tumor accepted hepatectomy between Jan 2006 and Dec 2009 from Xiangya Hospital were enrolled
97 cases of randomly selected liver tumor accepted hepatectomy between Jan 2005 and Dec 2008 from Affiliated Cancer Hospital were enrolled
45 excluded
27 cholangiocarcinoma
7 liver metastases
6 hepatic hemangioma
5 incomplete information
34 excluded
19 cholangiocarcinoma
5 liver metastases
4 hepatic hemangioma
6 incomplete information
Training cohort (n=100)
Validation cohort (n=63)
Immunohistochemistry
Immunohistochemistry
73casesof high ACTL6A expression
27 cases of low ACTL6A expression
43casesof high ACTL6A expression
20 cases of low ACTL6A expression
Correlation of ACTL6A expression with the clinicopathological characteristics and survival of HCC patients
Cox's proportional hazards regression model for univariate and multivariate analysis of risk factor
Prognostic value of ACTL6A for HCC patients

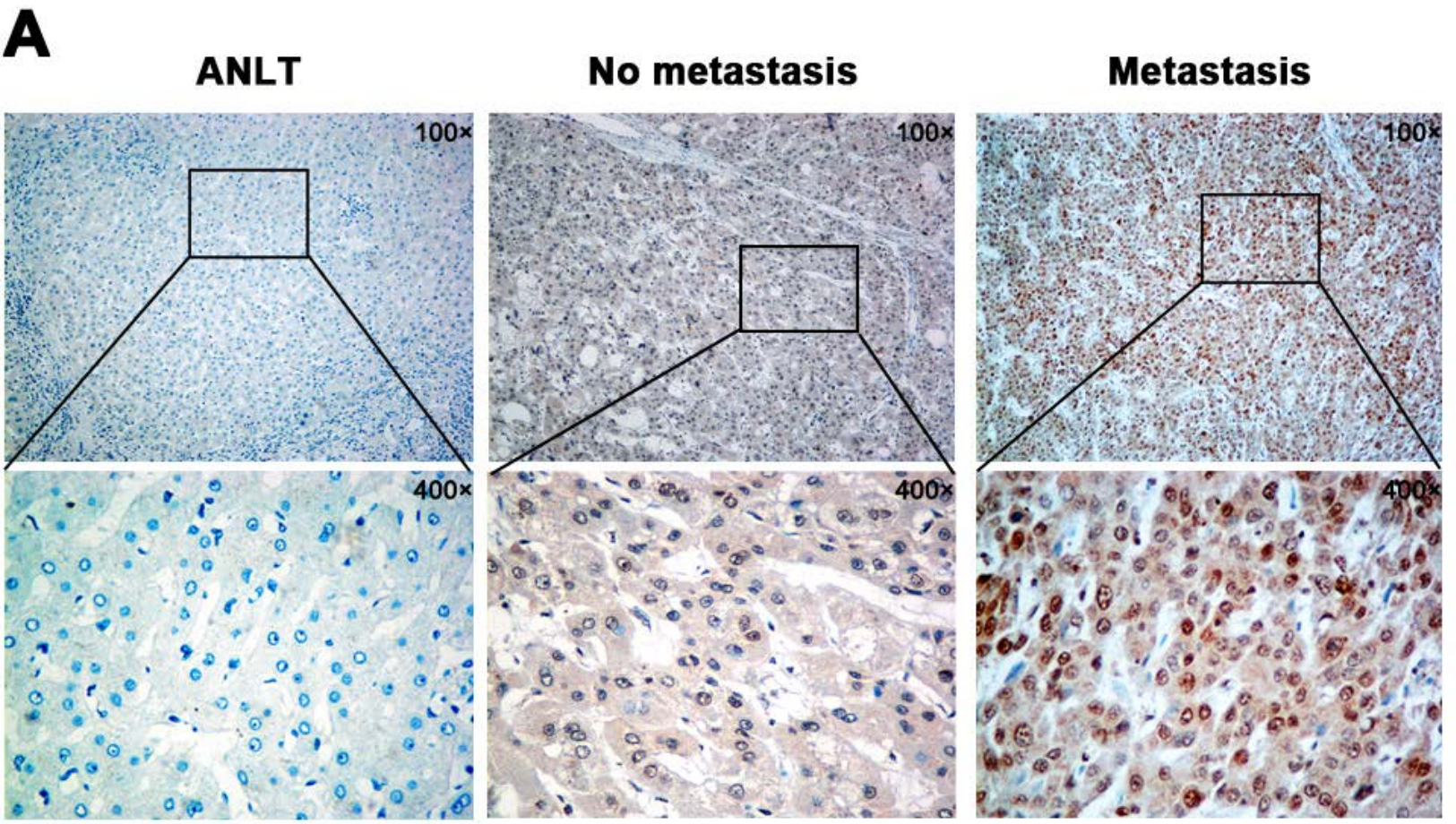
A
ANLT
No metastasis
Metastasis
100×
100×
100×
400×
400×
400×

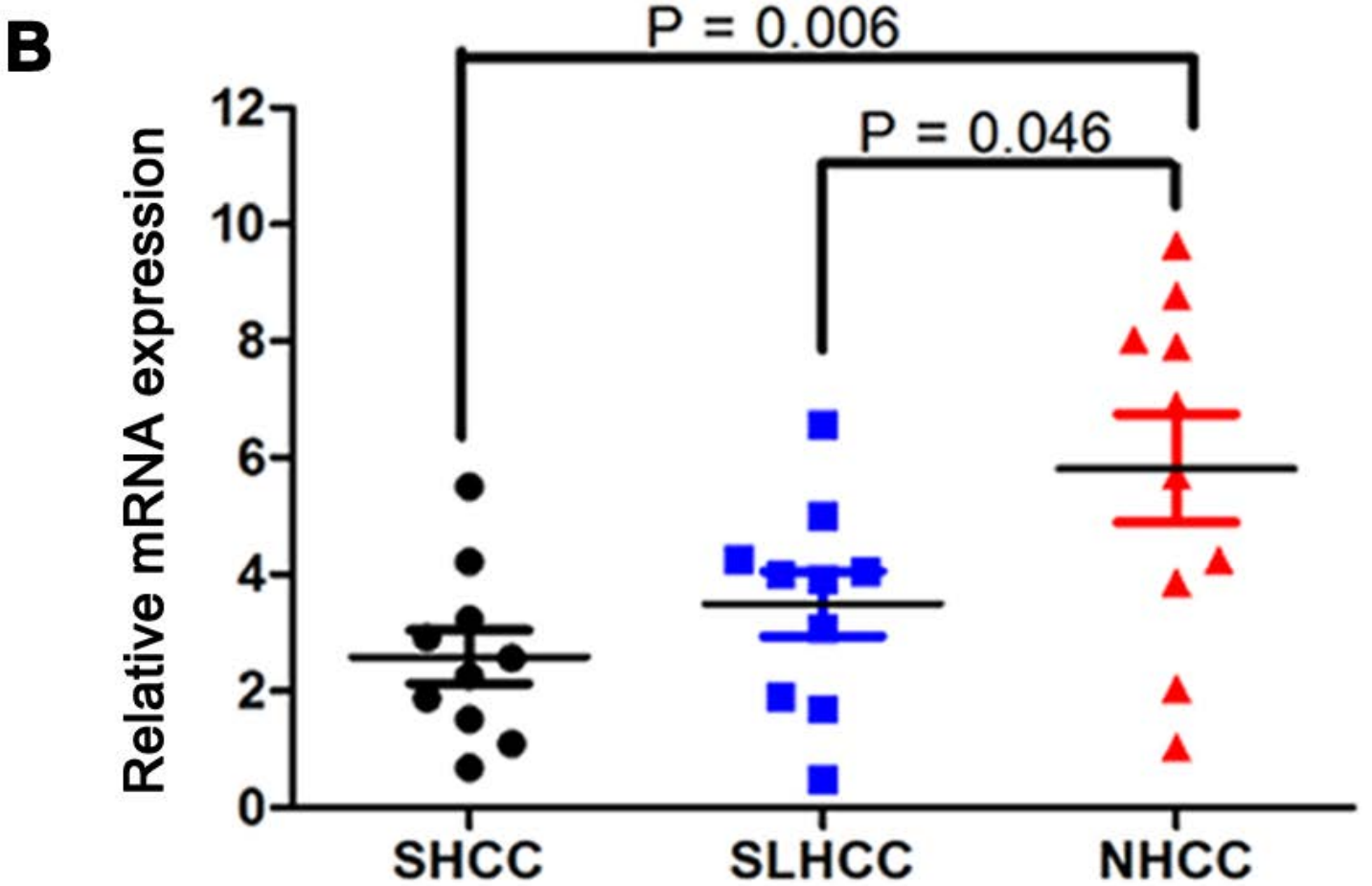
B
P = 0.006
P = 0.046
Relative mRNA expression
12
10
8
6
4
2
0
SHCC
SLHCC
NHCC

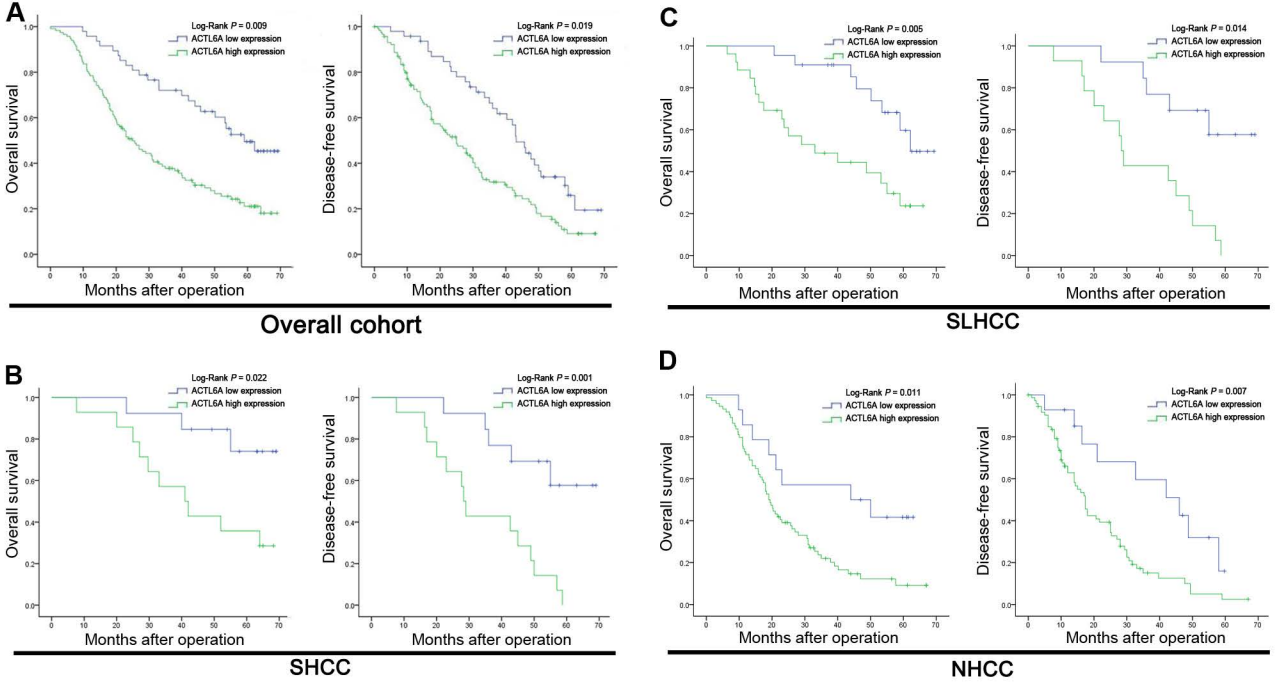
A
Log-Rank P = 0.009
ACTL6A low expression
ACTL6A high expression
Overall survival
Months after operation
Log-Rank P = 0.019
ACTL6A low expression
ACTL6A high expression
Disease-free survival
Months after operation
Overall cohort
B
Log-Rank P = 0.022
ACTL6A low expression
ACTL6A high expression
Overall survival
Months after operation
Log-Rank P = 0.001
ACTL6A low expression
ACTL6A high expression
Disease-free survival
Months after operation
SHCC
C
Log-Rank P = 0.005
ACTL6A low expression
ACTL6A high expression
Overall survival
Months after operation
Log-Rank P = 0.014
ACTL6A low expression
ACTL6A high expression
Disease-free survival
Months after operation
SLHCC
D
Log-Rank P = 0.011
ACTL6A low expression
ACTL6A high expression
Overall survival
Months after operation
Log-Rank P = 0.007
ACTL6A low expression
ACTL6A high expression
Disease-free survival
Months after operation
NHCC

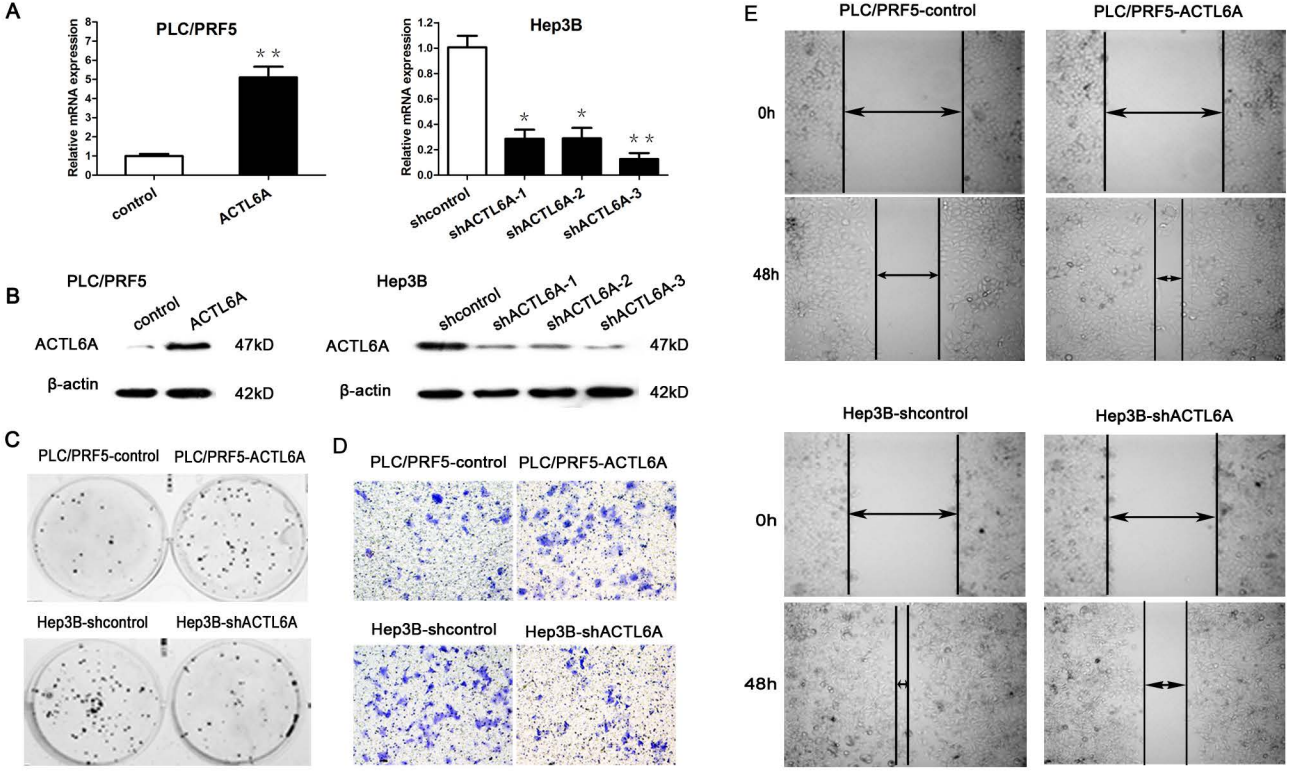
A
PLC/PRF5
Relative mRNA expression
control
ACTL6A
Hep3B
shcontrol
shACTL6A-1
shACTL6A-2
shACTL6A-3
B
PLC/PRF5
Hep3B
ACTL6A
47kD
β-actin
42kD
C
PLC/PRF5-control
PLC/PRF5-ACTL6A
Hep3B-shcontrol
Hep3B-shACTL6A
D
E
0h
48h

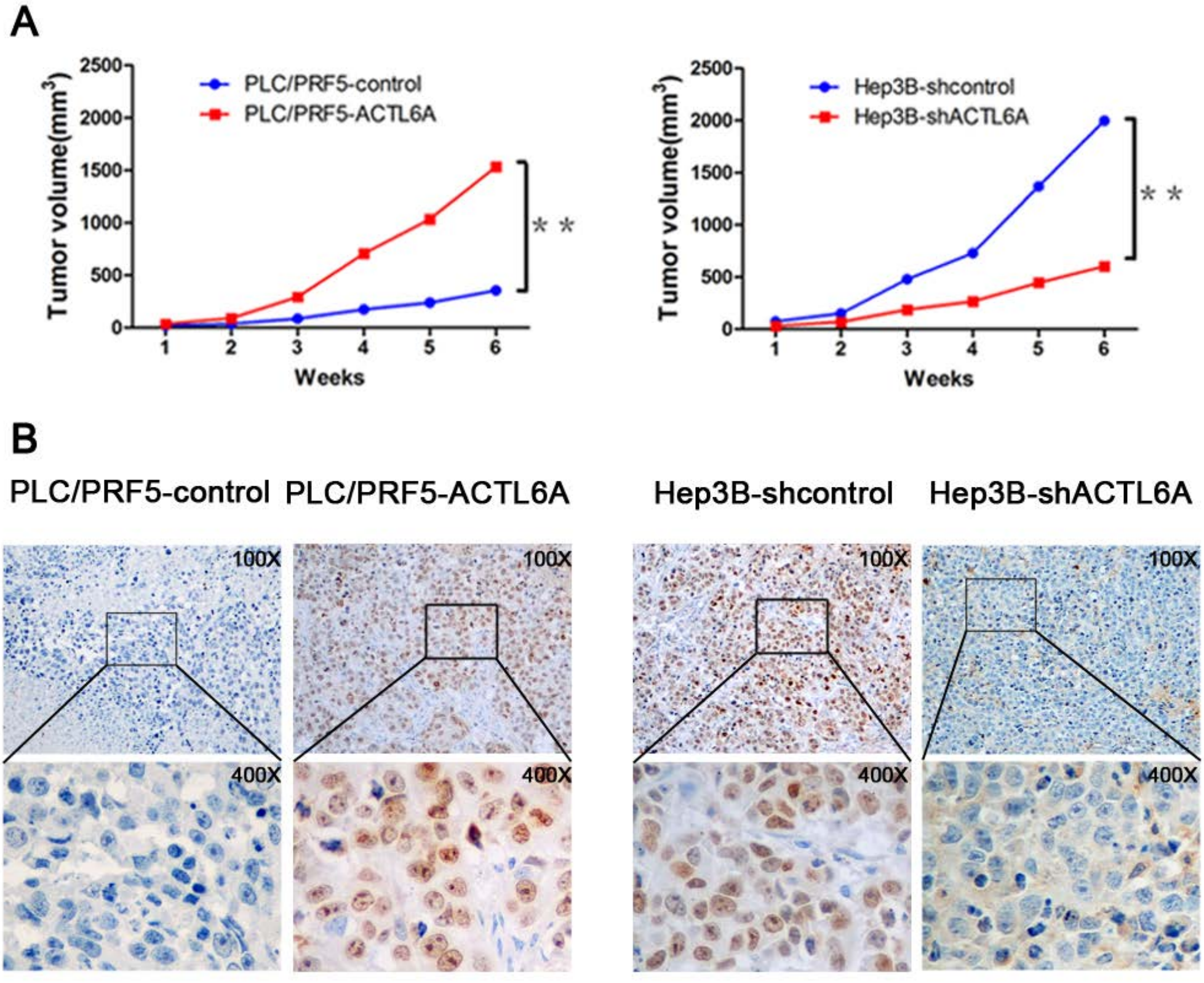
A
Tumor volume(mm3)
2500
2000
1500
1000
500
0
PLC/PRF5-control
PLC/PRF5-ACTL6A
1
2
3
4
5
6
Weeks
* *
Tumor volume(mm3)
Hep3B-shcontrol
Hep3B-shACTL6A
Weeks
* *
B
PLC/PRF5-control
PLC/PRF5-ACTL6A
Hep3B-shcontrol
Hep3B-shACTL6A
100X
400X

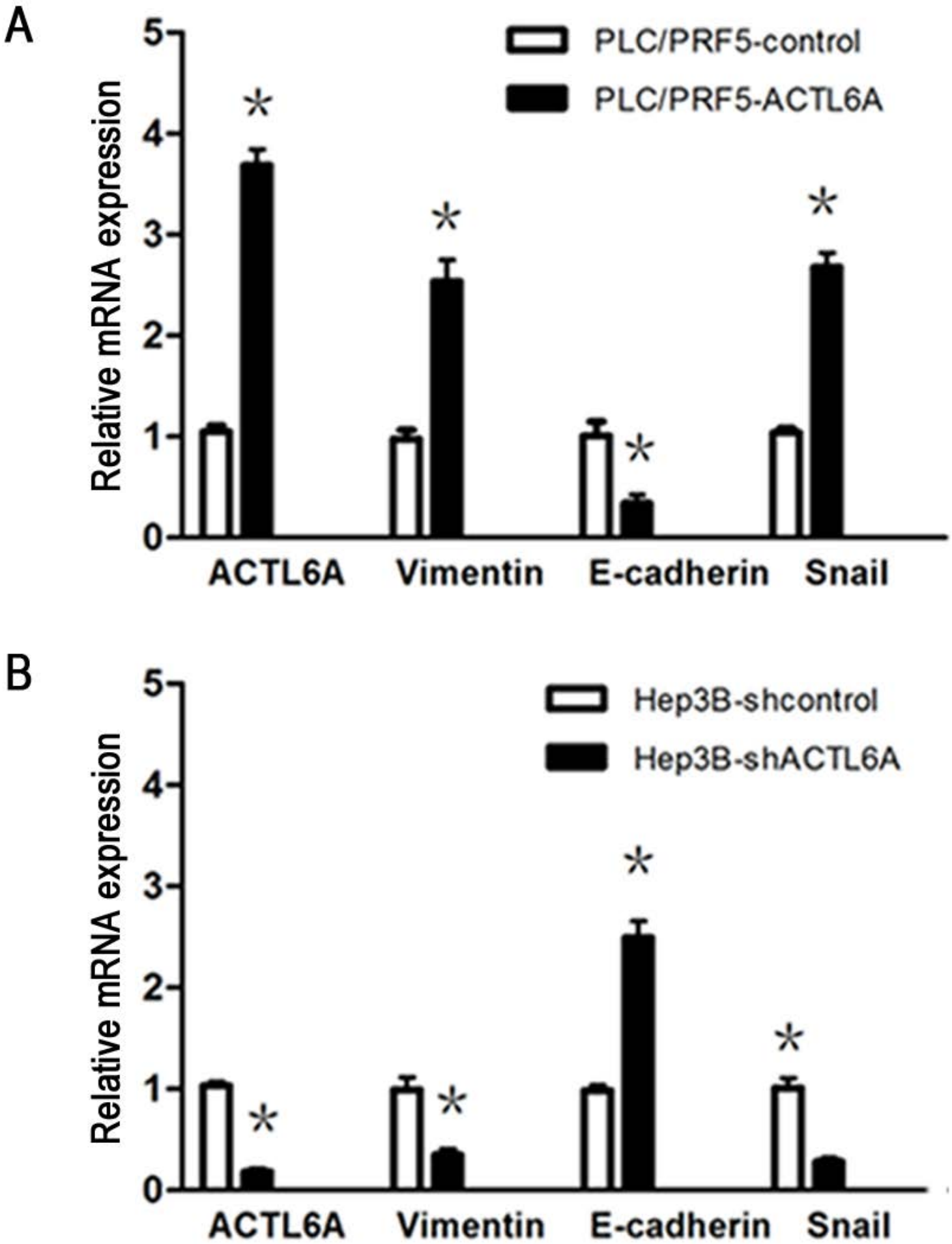
A
PLC/PRF5-control
PLC/PRF5-ACTL6A
Relative mRNA expression
0
1
2
3
4
5
*
*
*
*
ACTL6A
Vimentin
E-cadherin
Snail
B
Hep3B-shcontrol
Hep3B-shACTL6A
Relative mRNA expression
0
1
2
3
4
5
*
*
*
*
ACTL6A
Vimentin
E-cadherin
Snail

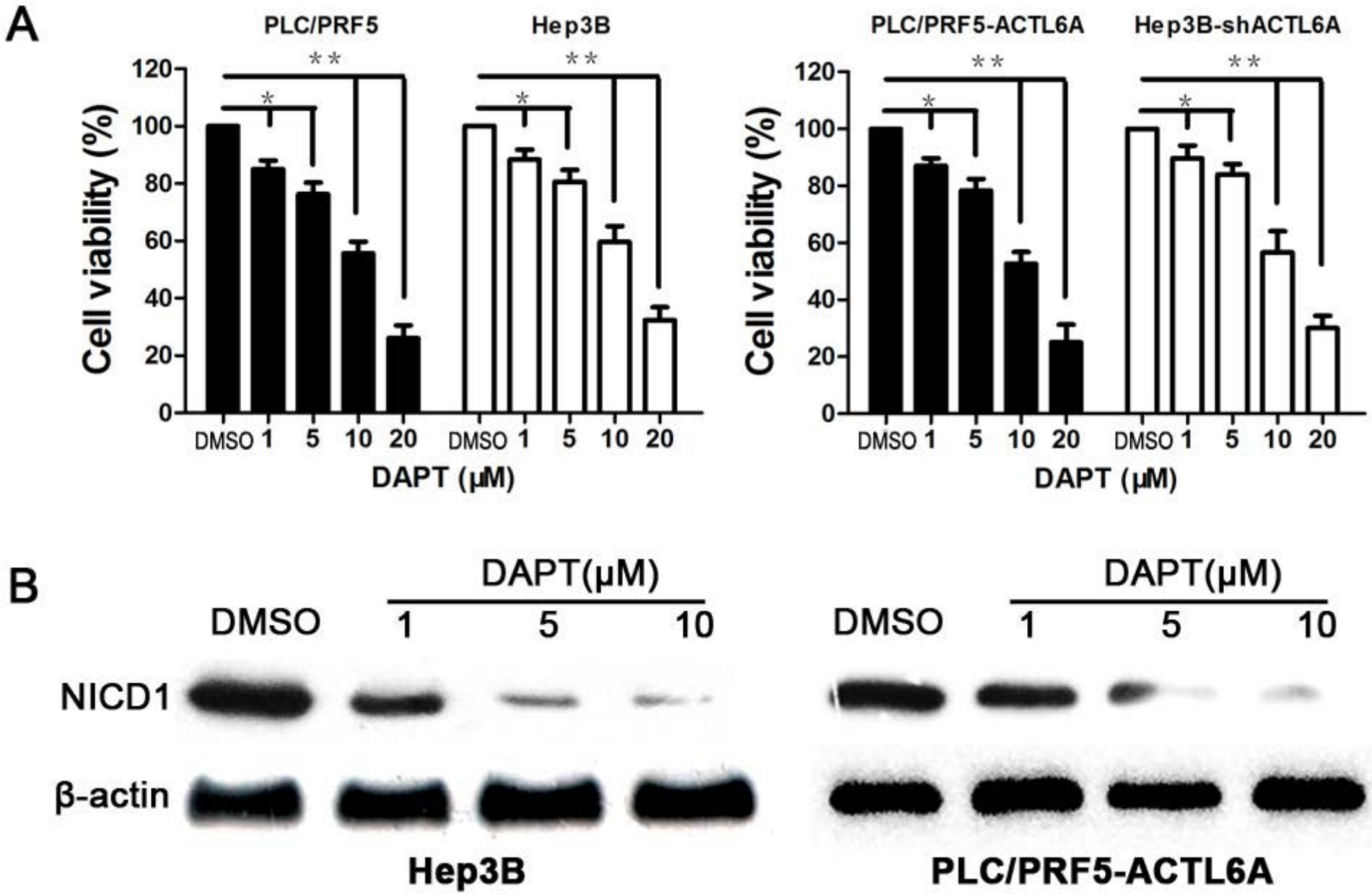
A
PLC/PRF5
Hep3B
PLC/PRF5-ACTL6A
Hep3B-shACTL6A
Cell viability (%)
120
100
80
60
40
20
0
* *
*
DMSO 1 5 10 20
DAPT (μM)
B
DAPT(μM)
DMSO
1
5
10
NICD1
β-actin
Hep3B
PLC/PRF5-ACTL6A

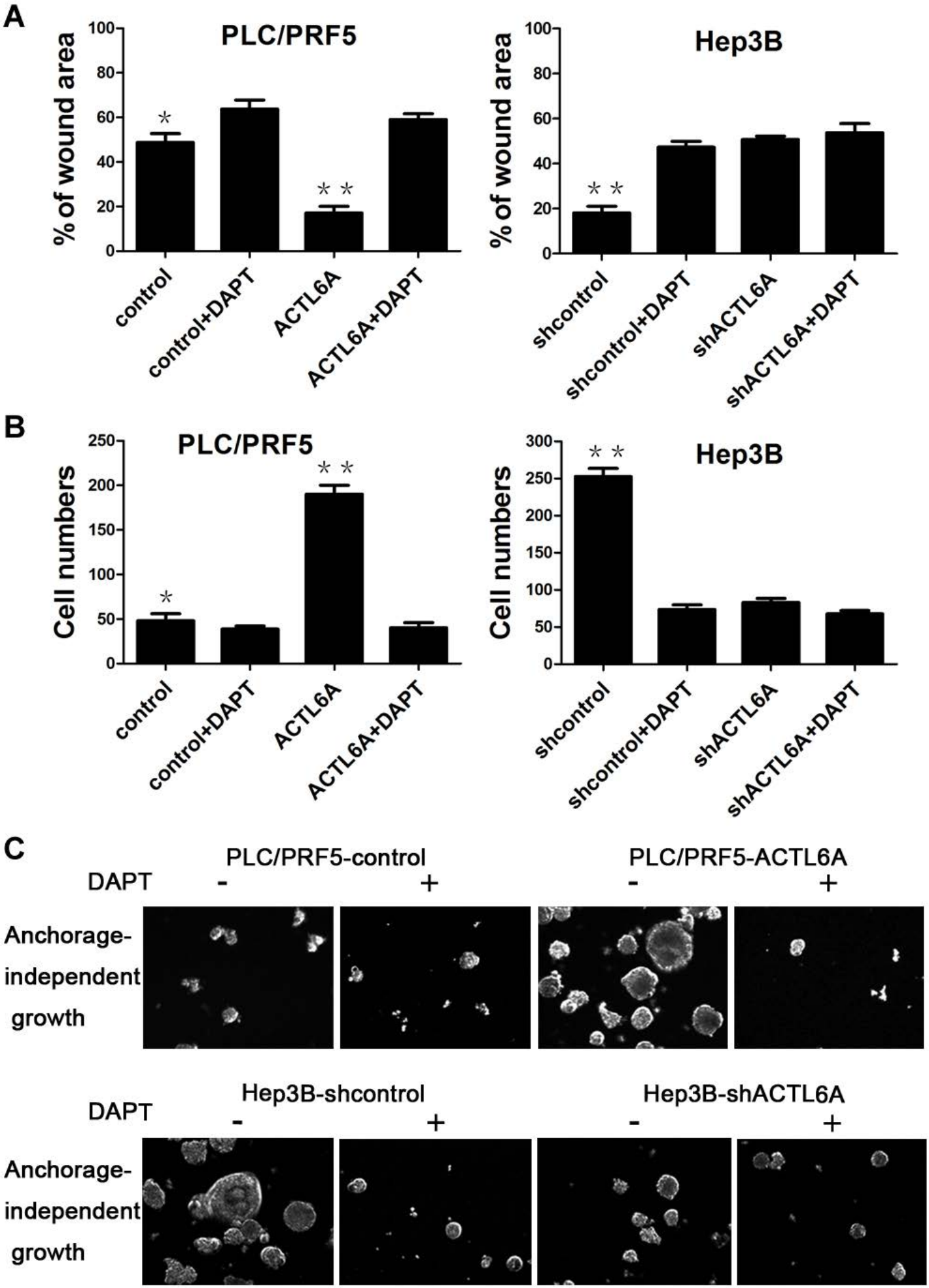
A
PLC/PRF5
% of wound area
100
80
60
40
20
0
*
* *
control
control+DAPT
ACTL6A
ACTL6A+DAPT
Hep3B
% of wound area
* *
shcontrol
shcontrol+DAPT
shACTL6A
shACTL6A+DAPT
B
PLC/PRF5
Cell numbers
250
200
150
100
50
0
* *
*
control
control+DAPT
ACTL6A
ACTL6A+DAPT
Hep3B
Cell numbers
300
250
200
150
100
50
0
* *
shcontrol
shcontrol+DAPT
shACTL6A
shACTL6A+DAPT
C
PLC/PRF5-control
DAPT
-
+
PLC/PRF5-ACTL6A
-
+
Anchorage-independent growth
Hep3B-shcontrol
DAPT
-
+
Hep3B-shACTL6A
-
+
Anchorage-independent growth

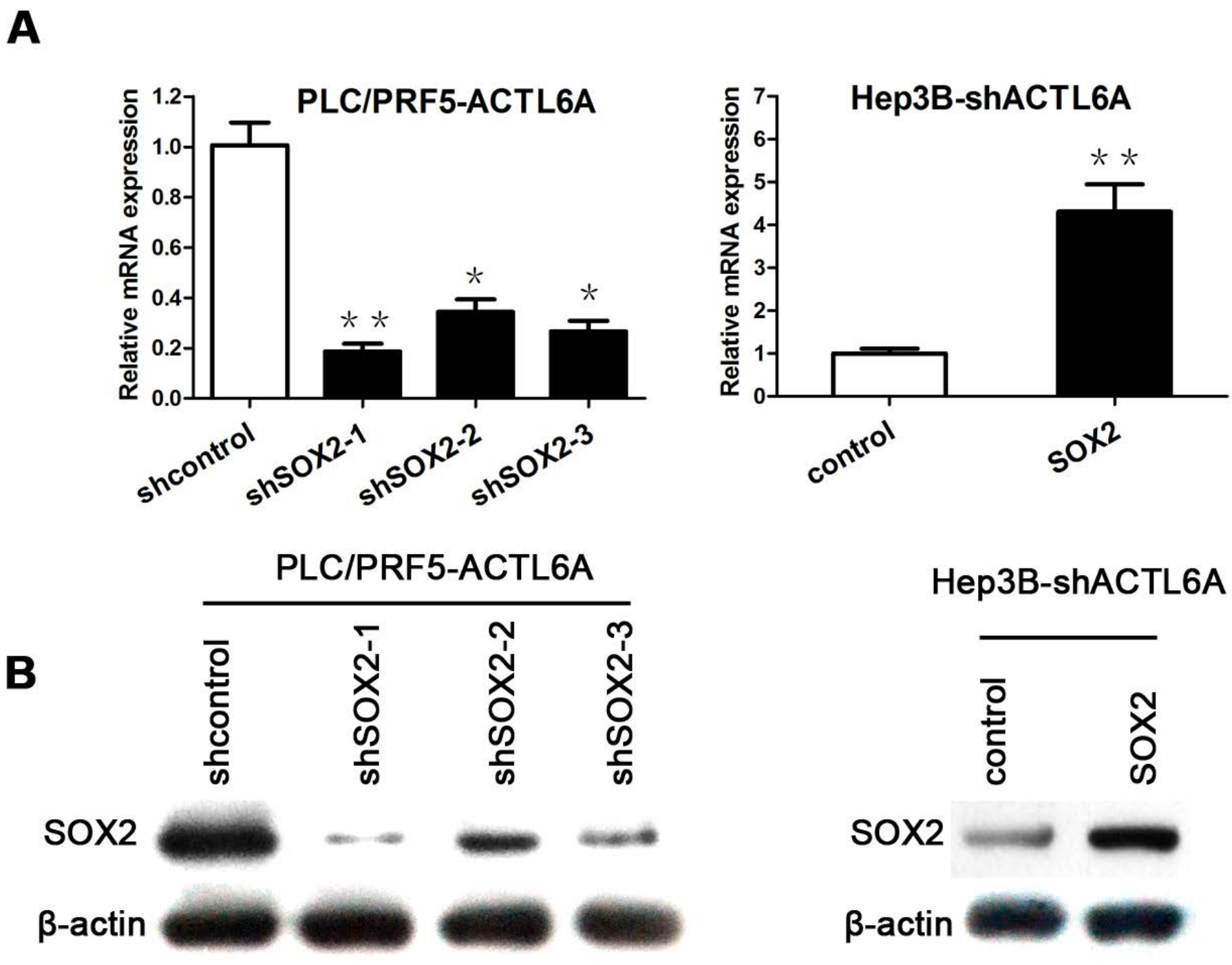
A
PLC/PRF5-ACTL6A
Relative mRNA expression
1.2
1.0
0.8
0.6
0.4
0.2
0.0
* *
*
*
shcontrol
shSOX2-1
shSOX2-2
shSOX2-3
Hep3B-shACTL6A
Relative mRNA expression
7
6
5
4
3
2
1
0
* *
control
SOX2
B
PLC/PRF5-ACTL6A
shcontrol
shSOX2-1
shSOX2-2
shSOX2-3
SOX2
β-actin
Hep3B-shACTL6A
control
SOX2
SOX2
β-actin

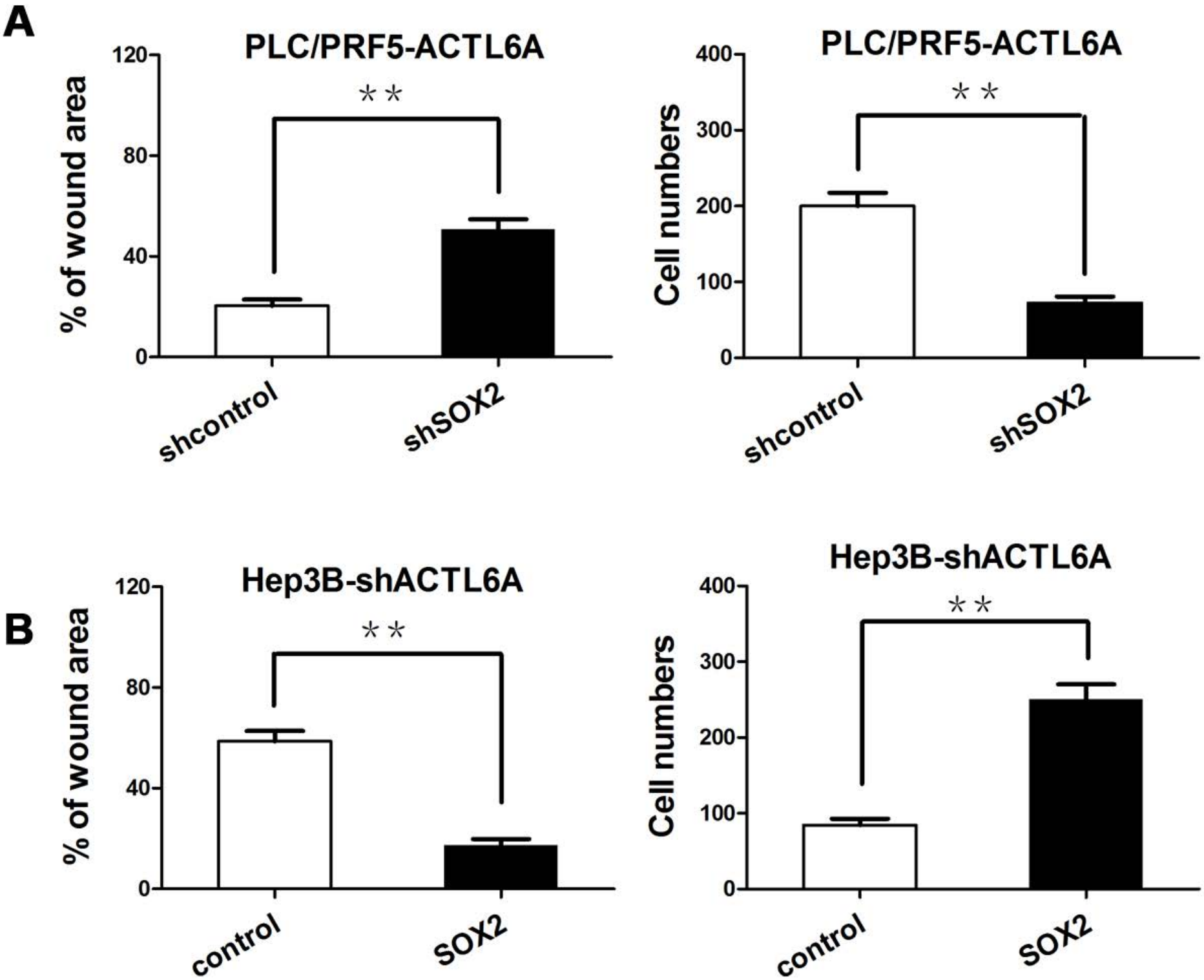
A
PLC/PRF5-ACTL6A
% of wound area
120
80
40
0
**
shcontrol
shSOX2
PLC/PRF5-ACTL6A
Cell numbers
400
300
200
100
0
**
shcontrol
shSOX2
B
Hep3B-shACTL6A
% of wound area
120
80
40
0
**
control
SOX2
Hep3B-shACTL6A
Cell numbers
400
300
200
100
0
**
control
SOX2

A

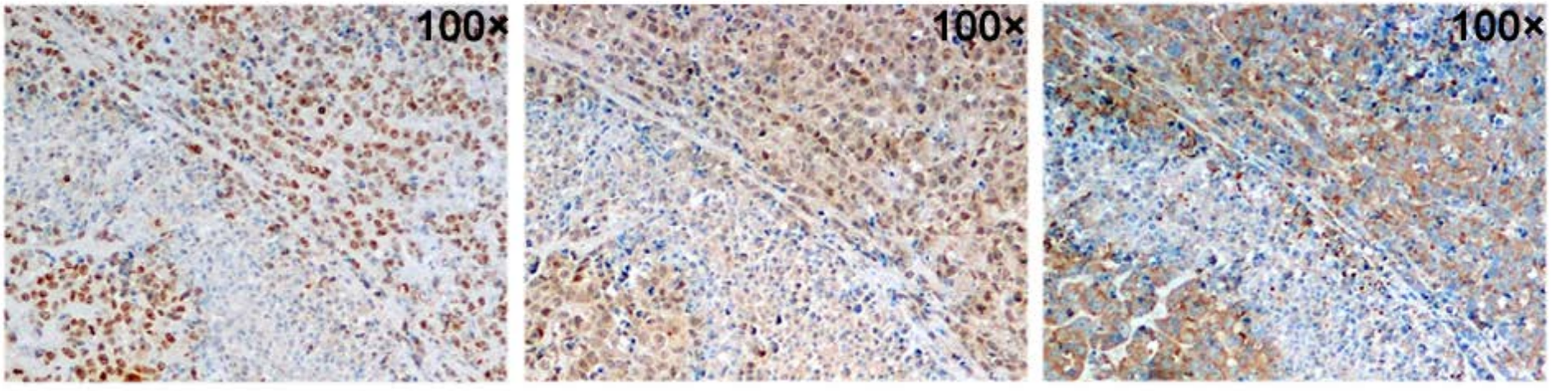

B

Training cohort

		ACTL6A expression		*P*	NICD1 expression		*P*
		High(73)	Low(27)	r	High(58)	Low(42)	r
SOX2	High(61)	52	9	＜0.01	45	16	＜0.01
expression	Low(39)	21	18	0.345	13	26	0.400

Validation cohort

		ACTL6A expression		*P*	NICD1 expression		*P*
		High(43)	Low(20)	r	High(41)	Low(22)	r
SOX2	High(38)	30	8	0.024	32	6	＜0.01
expression	Low(25)	13	12	0.283	9	16	0.495

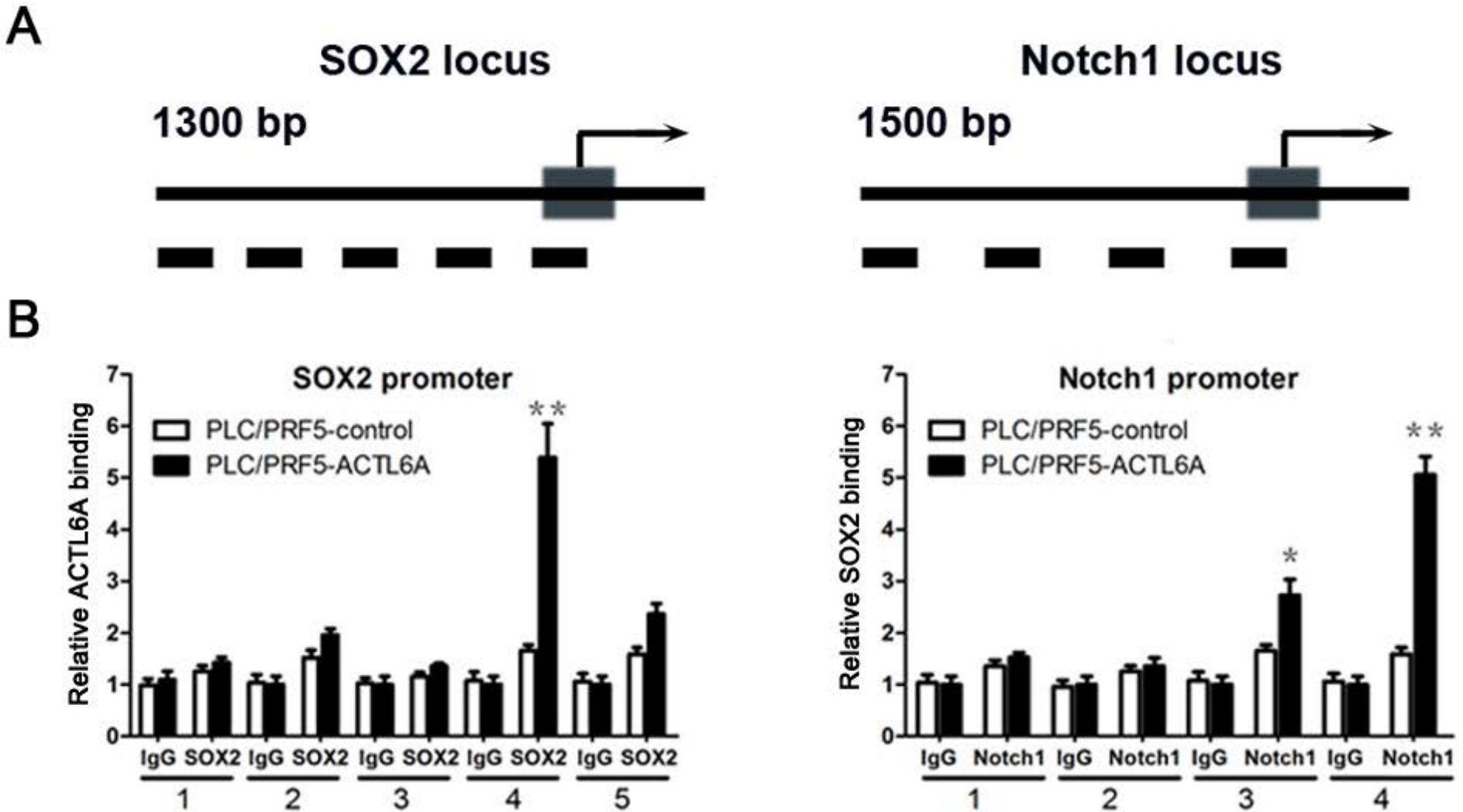
A
SOX2 locus
1300 bp
Notch1 locus
1500 bp
B
SOX2 promoter
PLC/PRF5-control
PLC/PRF5-ACTL6A
Relative ACTL6A binding
IgG SOX2 IgG SOX2 IgG SOX2 IgG SOX2 IgG SOX2
1 2 3 4 5
Notch1 promoter
Relative SOX2 binding
IgG Notch1 IgG Notch1 IgG Notch1 IgG Notch1
1 2 3 4

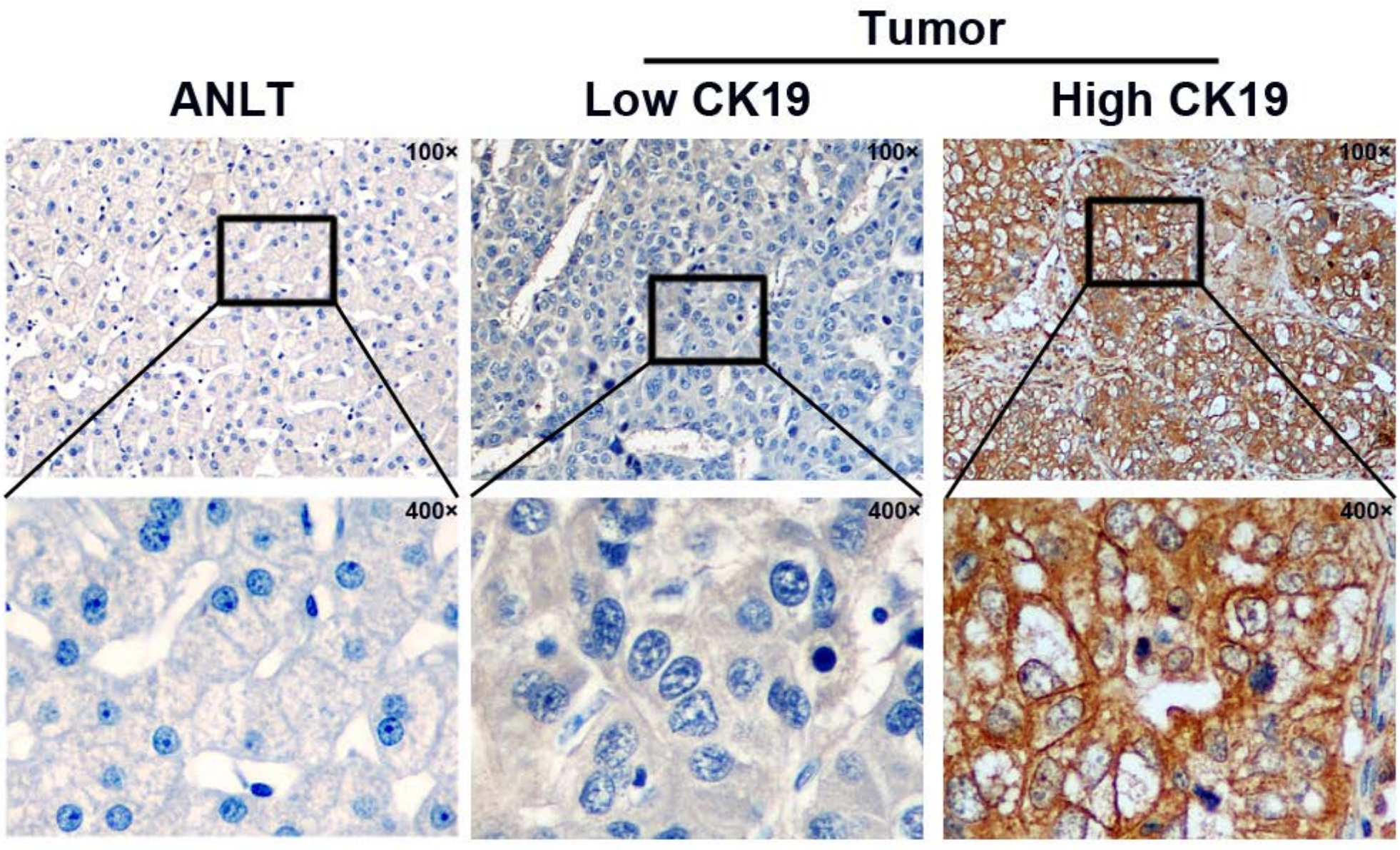
Tumor
ANLT
Low CK19
High CK19
100×
100×
100×
400×
400×
400×

Supplementary Tables

Supplementary Table 1. Clinicopathologcal characteristics of patients in training cohort and validation cohort

Clinicopathologic Variables	Counts		*P*
	Training cohort	Validation cohort	
Gender			
Female	31(31.0%)	22(34.9%)	
Male	69(69.0%)	41(65.1%)	0.603
Age			
<50	62(62.0%)	37(58.7%)	
≥50	38(38.0%)	26(41.3%)	0.677
AFP(ng/mL)			
<20	43(43.0%)	25(39.7%)	
≥20	57(57.0%)	38(60.3%)	0.676
HBsAg			
Negative	7(7.0%)	6(9.5%)	
Positive	93(93.0%)	57(90.5%)	0.563
Liver cirrhosis			
Absence	35(35.0%)	21(33.3%)	
Presence	65(65.0%)	42(66.6%)	0.827
Liver function			
Child-Pugh A	91(91.0%)	56(88.9%)	
Child-Pugh B	9(9.0%)	7(11.1%)	0.659
Tumor size(cm)			
≤5	38(38.0%)	19(30.2%)	
>5	62(62.0%)	44(69.8%)	0.307
Tumor nodule number			
Solitary	57(57.0%)	30(47.6%)	
Multiple(≥2)	43(43.0%)	33(52.4%)	0.242
Capsulation formation			
Presence	42(42.0%)	26(41.3%)	
Absence	58(58.0%)	37(58.7%)	0.927
Edmondson-Steiner grade			
Ⅰ&Ⅱ	64(64.0%)	39(62.0%)	
Ⅲ&Ⅳ	36(36.0%)	24(38.0%)	0.787
Microvascular invasion			
Absence	34(34.0%)	25(39.7%)	
Presence	66(66.0%)	38(60.3%)	0.462
BCLC stage			
0&A	28(28.0%)	18(28.6%)	
B&C	72(72.0%)	45(71.4%)	0.937
TNM stage			
Early (Ⅰ&Ⅱ)	67(67.0%)	35(55.6%)	
Late (Ⅲ&Ⅳ)	33(33.0%)	28(44.4%)	0.142

Abbreviations: AFP, alpha-fetoprotein; HBsAg, hepatitis B surface antigen; TNM, tumor node metastasis; BCLC, Barcelona Clinic Liver Cancer.

Supplementary Table 2. Univariate and multivariate Analysis of risk factors associated with overall survival of HCC patients in the validation cohort

Variables	n	Univariate analysis		Multivariate analysis	
		HR(95% CI)	*P*	HR(95% CI)	*P*
Gender					
Female	22	1			
Male	41	1.157(0.459-1.817)	0.568	NA	
Age					
<50	37	1			
≥50	26	1.237(0.764-1.404)	0.313	NA	
AFP(ng/mL)					
<20	25	1			
≥20	38	1.341(0.248-2.325)	0.221	NA	
HBsAg					
Negative	6	1			
Positive	57	1.328(0.819-1.614)	0.174	NA	
Liver cirrhosis					
Absence	21	1		1	
Presence	42	2.217(1.293-3.127)	**0.003**	1.873(1.126-2.619)	**0.011**
Liver function					
Child-Pugh A	56	1			
Child-Pugh B	7	2.138(1.147-3.975)	**0.018**	NS	
Tumor size(cm)					
≤5	19	1			
>5	44	1.418(0.735-1.866)	0.283	NA	
Tumor nodule number					
Solitary	30	1		1	
Multiple(≥2)	33	3.261(1.434-5.293)	**<0.001**	2.465(1.332-3.646)	**0.008**
Capsulation formation					
Presence	26	1			
Absence	37	1.217(0.614-1.895)	0.098	NS	
Edmondson-Steiner grade					
Ⅰ&Ⅱ	39	1			
Ⅲ&Ⅳ	24	1.796(1.154-2.563)	**0.023**	NS	
Microvascular invasion					
Absence	25	1		1	
Presence	38	3.468(1.936-5.458)	**<0.001**	2.815(1.274-4.502)	**0.007**
BCLC stage					
0&A	18	1		1	
B&C	45	3.216(1.362-5.074)	**<0.001**	2.194(1.358-3.463)	**0.014**
TNM stage					
Early (Ⅰ&Ⅱ)	35	1		1	
Late (Ⅲ&Ⅳ)	28	4.271(1.853-6.732)	**<0.001**	3.276(1.548-5.292)	**0.001**
ACTL6A expression					

Low	20	1		1	
High	43	2.318(1.414-3.329)	**0.008**	2.596(1.641-3.692)	**0.011**

Supplementary Table 3. Univariate and multivariate Analysis of risk factors associated with disease-free survival of HCC patients in the validation cohort

Variables		Univariate analysis		Multivariate analysis	
	n	HR(95% CI)	*P*	HR(95% CI)	*P*
Gender					
Female	22	1			
Male	41	1.036(0.543-1.417)	0.782	NA	
Age					
<50	37	1			
≥50	26	1.132(0.652-1.707)	0.541	NA	
AFP(ng/mL)					
<20	25	1			
≥20	38	1.915(1.077-3.314)	**0.022**	NS	
HBsAg					
Negative	6	1			
Positive	57	1.725(0.745-3.411)	0.119	NA	
Liver cirrhosis					
Absence	21	1			
Presence	42	2.436(1.392-3.641)	**0.002**	NS	
Liver function					
Child-Pugh A	56	1			
Child-Pugh B	7	1.638(0.854-2.523)	0.173	NA	
Tumor size(cm)					
≤5	19	1			
>5	44	1.325(0.619-1.736)	0.217	NA	
Tumor nodule number					
Solitary	30	1		1	
Multiple(≥2)	33	2.814(1.658-4.731)	**0.001**	2.172(1.132-3.374)	**0.008**
Capsulation formation					
Presence	26	1			
Absence	37	1.754(1.193-2.618)	**0.038**	NS	
Edmondson-Steiner grade					
Ⅰ&Ⅱ	39	1			
Ⅲ&Ⅳ	24	1.934(1.211-2.754)	**0.006**	NS	
Microvascular invasion					
Absence	25	1		1	
Presence	38	3.945(2.144-5.912)	**<0.001**	3.183(1.765-4.682)	**0.015**
BCLC stage					
0&A	18	1		1	
B&C	45	2.923(1.721-5.392)	**0.001**	2.468(1.493-4.572)	**0.003**

TNM stage					
Early (Ⅰ&Ⅱ)	35	1		1	
Late (Ⅲ&Ⅳ)	28	4.173(1.925-6.735)	**<0.001**	2.852(1.417-4.275)	**0.001**
ACTL6A expression					
Low	20	1		1	
High	43	2.693(1.417-4.027)	**0.004**	2.118(1.342-3.147)	**0.009**

Supplementary Table 4. The sequences of PCR primers and RNAi used in this study

Target gene	Application	Sequence
ACTL6A	RT-PCR	F: GGTCGTTCTACTGGGCTGATT
		R: AGCAAGAGGGGATTTCACAAT
ACTL6A	real-time PCR	F: CCAGGTCTCTATGGCAGTGTAA
		R: CGTAAGGTGACAAAAGGAAGGTA
GAPDH	RT-PCR	F: AGAAGGCTGGGGCTCATTTG
		R: AGGGGCCATCCACAGTCTTC
GAPDH	real-time PCR	F: GTCTCCTCTGACTTCAACAGCG
		R: ACCACCCTGTTGCTGTAGCCAA
Notch1	real-time PCR	F: GGTGAACTGCTCTGAGGAGATC
		R: GGATTGCAGTCGTCCACGTTGA
Notch2	real-time PCR	F: GTGCCTATGTCCATCTGGATGG
		R: AGACACCTGAGTGCTGGCACAA
Notch3	real-time PCR	F: TACTGGTAGCCACTGTGAGCAG
		R: CAGTTATCACCATTGTAGCCAGG
Notch4	real-time PCR	F: TTCCACTGTCCTCCTGCCAGAA
		R: TGGCACAGGCTGCCTTGGAATC
Jagged1	real-time PCR	F: CAACGGCGAGTCCTTTAC
		R: CTGGCATTCATTGATGTTTA
SOX2	real-time PCR	F: CGCAGACCTACATGAACG

		R: CCCTGGAGTGGGAGGAA
Hes1	real-time PCR	F: GGTGGCTGCTACCCCAGCCA
		R: GGTAGGTCATGGCGTTGATC
E-cadherin	real-time PCR	F: GCCTCCTGAAAAGAGAGTGGAAG
		R: TGGCAGTGTCTCTCCAAATCCG
Vimentin	real-time PCR	F: AGGCAAAGCAGGAGTCCACTGA
		R: ATCTGGCGTTCCAGGGACTCAT
Snail	real-time PCR	F: TGCCCTCAAGATGCACATCCGA
		R: GGGACAGGAGAAGGGCTTCTC

Supplementary Table 5. List of the Antibodies used in this study.

Antibody name	Source
ACTL6A	Santa Cruz (sc-137062)
β-actin	Sigma Aldrich (A5316)
E-cadherin	Santa Cruz (sc-7870)
Vimentin	Santa Cruz (sc-7557)
Snail	Abcam (ab85936)
Jagged1	Cell signaling (2620)
Notch1	Santa Cruz (sc-23299)
RBP-Jκ	Santa Cruz (sc-28713)
Hes1	Santa Cruz (sc-166410)
SOX2	Abcam (ab92494)
Cytokeratin 19	Proteintech(60187-1-Ig)

Supplementary Table 6. List of the reagents used in this study.

Reagent name	Source
Donkey anti-Mouse IgG (H+L) Cross Adsorbed Secondary Antibody, DyLight 594 conjugate	ThermoFisher Scientific (SA5-10168)
Donkey anti-Rabbit IgG (H+L) Cross Adsorbed Secondary Antibody, DyLight 488 conjugate	ThermoFisher Scientific (SA5-10038)
Donkey anti-Goat IgG (H+L) Cross Adsorbed Secondary Antibody, DyLight 650 conjugate	ThermoFisher Scientific (SA5-10089)
Goat anti-Rabbit IgG (H+L) Secondary Antibody, DyLight 594 conjugate	ThermoFisher Scientific (# 35560)
Donkey anti-Goat IgG (H+L) Cross Adsorbed Secondary Antibody, DyLight 594 conjugate	ThermoFisher Scientific (SA5-10088)
DAPT (GSI-IX)	Selleck (S2215)
CellTiter 96® AQueous One Solution Cell Proliferation Assay	Promega (G3582)
Mitomycin C	Roche (M8170)
EpiQuikTM Chromatin Immunoprecipitation Kit	Epigentek (P-2002)
Polymer HRP Detection System	ZSGB-BIO (PV-9000, PV-9003)
Cignal Finder Cancer 10-Pathway Reporter Array	QIAGEN (CCA-101L)

Supplementary Table 7. The primers used for CHIP-qPCR in this study

CHIP-qPCR region	Forward primer	Reverse primer
SOX2-1	CCTCCATACAGTGCCGTGGGA	GTAAGAAGGGTTTCGGTCGTG
SOX2-2	TTGCTACGGTTGAATGAAGAC	TTCCACGTAACTTGCTCTGTT
SOX2-3	CTTCTAGTCGGGACTGTGAGA	GGTGCAGGGTACTTAAATGAG
SOX2-4	GATGAGCGGGAGAACAATGAC	CAGCACTAAGACTACGTGGGT
SOX2-5	CCCGTCACATGGATGGTTGTC	CCGCCGCCGATGATTGTTATT
Notch1-1	CCTCCCAGCCTTTCGGTCTCC	CCCTGTGCCAAGCCTGGTTAA
Notch1-2	CGCCTTCTGCCATCGCACTCA	CGTGCTCCTTCCGGCTGATTT
Notch1-3	AGATCCGCCCGACCCGTTTGT	CGTGATTGCCCGAGCACTTGA
Notch1-4	ACGGTGCCCGAGGAGCGTGTC	CACTTGACCGCGAGGGATGGG

Supplementary Table 8. The sequences of RNAi and cDNA clone used in this study

Name	Sequence
ACTL6A-RNAi-1	TCCAAGTATGCGGTTGAAA
ACTL6A-RNAi-2	GTACTTCAAGTGTCAGATT
ACTL6A-RNAi-3	GGGATAGTTTCCAAGCTAT
SOX2-RNAi-1	GTTCTAGTGGTACGGTAGG
SOX2-RNAi-2	AGTTCTAGTGGTACGGTAG
SOX2-RNAi-3	TCAGTCTGCCGAGAATCCA
ORF Nucleotide Sequence of ACTL6A	CGAAGCTTGGGCTGCAGGTCGACTCTAGAGGATCCC CGGGTACCGGTCGCCACCATGAGCGGCGGCGTGTAC GGGGGAGATGAAGTTGGAGCCCTTGTTTTTGACATTG GATCCTATACTGTGAGAGCTGGTTATGCTGGTGAGGA CTGCCCCAAGGTGGATTTTCCTACAGCTATTGGTATGG TGGTAGAAAGAGATGACGGAAGCACATTAATGGAAATA GATGGCGATAAAGGCAAACAAGGCGGTCCCACCTACT ACATAGATACTAATGCTCTGCGTGTTCCGAGGGAGAAT ATGGAGGCCATTTCACCTCTAAAAAATGGGATGGTTGA AGACTGGGATAGTTTCCAAGCTATTTTGGATCATACCT ACAAAATGCATGTCAAATCAGAAGCCAGTCTCCATCCT GTTCTCATGTCAGAGGCACCGTGGAATACTAGAGCAA AGAGAGAGAAACTGACAGAGTTAATGTTTGAACACTA CAACATCCCTGCCTTCTTCCTTTGCAAAACTGCAGTTT TGACAGCATTTGCTAATGGTCGTTCTACTGGGCTGATT TTGGACAGTGGAGCCACTCATACCACTGCAATTCCAG TCCACGATGGCTATGTCCTTCAACAAGGCATTGTGAAA TCCCCTCTTGCTGGAGACTTTATTACTATGCAGTGCAG AGAACTCTTCCAAGAAATGAATATTGAATTGGTTCCTC CATATATGATTGCATCAAAAGAAGCTGTTCGTGAAGGA TCTCCAGCAAACTGGAAAAGAAAAGAGAAGTTGCCTC AGGTTACGAGGTCTTGGCACAATTATATGTGTAATTGT GTTATCCAGGATTTTCAAGCTTCGGTACTTCAAGTGTC AGATTCAACTTATGATGAACAAGTGGCTGCACAGATGC CAACTGTTCATTATGAATTCCCCAATGGCTACAATTGT GATTTTGGTGCAGAGCGGCTAAAGATTCCAGAAGGAT

	TATTTGACCCTTCCAATGTAAAGGGGTTATCAGGAAAC ACAATGTTAGGAGTCAGTCATGTTGTCACCACAAGTGT TGGGATGTGTGATATTGACATCAGACCAGGTCTCTATG GCAGTGTAATAGTGGCAGGAGGAAACACACTAATACA GAGTTTTACTGACAGGTTGAATAGAGAGCTGTCTCAG AAAACTCCTCCAAGTATGCGGTTGAAATTGATTGCAAA TAATACAACAGTGGAACGGAGGTTTAGCTCATGGATTG GCGGCTCCATTCTAGCCTCTTTGGGTACCTTTCAACA GATGTGGATTTCCAAGCAAGAATATGAAGAAGGAGGG AAGCAGTGTGTAGAAAGAAAATGCCCTGGTATGGACT ACAAGGATGACGATGACAAGGATTACAAAGACGACGA TGATAAGGACTATAAGGATGATGACGACAAATGAGCTA GCCTGTGGAA
ORF Nucleotide Sequence of SOX2	TTTTGTAATACGACTCACTATAGGGCGGCCGGGAATTC GTCGACTGGATCCGGTACCGAGGAGATCTGCCGCCG CGATCGCCATGTACAACATGATGGAGACGGAGCTGAA GCCGCCGGGCCCGCAGCAAACTTCGGGGGGCGGCG GCGGCAACTCCACCGCGGCGGCGGCCGGCGGCAAC CAGAAAAACAGCCCGGACCGCGTCAAGCGGCCCATG AATGCCTTCATGGTGTGGTCCCGCGGGCAGCGGCGC AAGATGGCCCAGGAGAACCCCAAGATGCACAACTCG GAGATCAGCAAGCGCCTGGGCGCCGAGTGGAAACTT TTGTCGGAGACGGAGAAGCGGCCGTTCATCGACGAG GCTAAGCGGCTGCGAGCGCTGCACATGAAGGAGCAC CCGGATTATAAATACCGGCCCCGGCGGAAAACCAAGA CGCTCATGAAGAAGGATAAGTACACGCTGCCCGGCG GGCTGCTGGCCCCCGGCGGCAATAGCATGGCGAGCG GGGTCGGGGTGGGCGCCGGCCTGGGCGCGGGCGT GAACCAGCGCATGGACAGTTACGCGCACATGAACGG CTGGAGCAACGGCAGCTACAGCATGATGCAGGACCA GCTGGGCTACCCGCAGCACCCGGGCCTCAATGCGCA CGGCGCAGCGCAGATGCAGCCCATGCACCGCTACGA CGTGAGCGCCCTGCAGTACAACTCCATGACCAGCTC GCAGACCTACATGAACGGCTCGCCCACCTACAGCATG TCCTACTCGCAGCAGGGCACCCCTGGCATGGCTCTT GGCTCCATGGGTTCGGTGGTCAAGTCCGAGGCCAGC TCCAGCCCCCCTGTGGTTACCTCTTCCTCCCACTCCA GGGCGCCCTGCCAGGCCGGGGACCTCCGGGACATG ATCAGCATGTATCTCCCCGGCGCCGAGGTGCCGGAA CCCGCCGCCCCCAGCAGACTTCACATGTCCCAGCAC TACCAGAGCGGCCCGGTGCCCGGCACGGCCATTAAC GGCACACTGCCCCTCTCACACATGACGCGTACGCGG CCGCTCGAGCAGAAACTCATCTCAGAAGAGGATCTGG

	CAGCAAATGATATCCTGGATTACAAGGATGACGACGATAAGGTTTAA

Supplementary Table 9. Correlation between CK19 expression with clinicopathological characteristics of HCC and ACTL6A expression in training cohort.

Clinicopathologic Variables	CK19 Expression			*P*
	n	Positive(17)	Negative(83)	
Gender				
Female	31	5	26	
Male	69	12	57	0.877
Age				
<50	62	10	52	
≥50	38	7	31	0.767
AFP(ng/mL)				
<20	43	9	34	
≥20	57	8	49	0.364
HBsAg				
Negative	7	3	4	
Positive	93	14	79	0.172
Liver cirrhosis				
Absence	35	6	29	
Presence	65	11	54	0.978
Liver function				
Child-Pugh A	91	15	76	
Child-Pugh B	9	2	7	0.662
Tumor size(cm)				
≤5	38	6	32	
>5	62	11	51	0.801
Tumor nodule number				
Solitary	57	4	53	

Multiple(≥2)	43	13	30	**0.001**
Capsulation formation				
Presence	42	6	36	
Absence	58	11	47	0.539
Edmondson-Steiner				
Ⅰ&Ⅱ	64	5	59	
Ⅲ&Ⅳ	36	12	24	**< 0.001**
Microvascular invasion				
Absence	34	4	30	
Presence	66	13	53	0.200
BCLC stage				
0&A	28	5	23	
B&C	72	12	60	0.887
TNM stage				
Early (Ⅰ&Ⅱ)	67	10	57	
Late (Ⅲ&Ⅳ)	33	7	26	0.431
ACTL6A expression				
High	73	11	62	
Low	27	6	21	0.398